

Error Performance of MIMO Systems in Frequency Selective Rayleigh Fading Channels

Huaping Liu

School of Electrical Engineering and Computer Science
Oregon State University, Corvallis, OR 97331 USA
Email: hliu@ece.orst.edu, Telephone: +1 541 737 2973

Abstract—This paper analyzes the error performance of multiple-input multiple-output (MIMO) systems in frequency-selective Rayleigh fading channels. A zero-forcing (ZF) receiver is applied to separate transmitted data streams for each resolvable multipath component. The decision for each symbol of a transmitted data stream is based on combining L zero-forced multipath components carrying information of the same symbol. Analytical error rate expressions for the system in the absence of inter-symbol interference (ISI) and inter-path interference (IPI) are derived first. Then, the effects of ISI and IPI caused by frequency-selective fading of the performance of a MIMO system with direct-sequence spreading applied to each transmitted symbol are studied by simulations. It is found that for a system with N transmit antennas, M receive antennas, and L resolvable multipath components, the ZF receiver combined with a RAKE with maximal ratio combining is equivalent to a 2-dimensional RAKE with a diversity order of $(M - N + 1)L$.

I. INTRODUCTION

Multiple receiving antennas have been used in the reverse link of mobile communication systems to suppress or cancel interference [1], [2]. Multiple-input multiple-output (MIMO) systems [3]–[9] have been shown to provide high spectral efficiencies. Existing research on MIMO techniques has focused mostly on capacity analysis and signal processing techniques for frequency nonselective Rayleigh fading channels. In the area of capacity analysis, significant research efforts (e.g., [3]–[5]) have been dedicated to exploring the ultimate theoretical capacity limit of MIMO systems in flat Rayleigh fading channels. It has been shown that in slowly-fading flat Rayleigh channels with mutually independent transmit and receive antennas, channel capacity grows linearly with the minimum number of antenna elements at either the transmitter or the receiver end. In the area of signal processing and performance analysis, error rate upper bounds of MIMO systems in frequency nonselective Rayleigh fading channel have been derived in [1] [9]. Based on these bounds, it was concluded that with M receive antennas for $N(N \leq M)$ simultaneously transmitted data streams through an independent matrix channel, appropriate signal processing schemes such as a zero-forcing (ZF) scheme or a minimum mean square error (MMSE) scheme can completely separate the N streams of data and at the same time achieve a $(M - N + 1)$ -order path diversity for each of the N streams of data.

In this paper, we study the performance of MIMO systems in frequency-selective Rayleigh fading channels. A zero-forcing receiver [9] is applied to separate the spatially multiplexed data on a path-by-path basis. A maximal ratio combiner

is then used to combine the zero-forced resolvable paths carrying information of the same transmitted symbol and form the decision statistics. System and channel models are provided in Section II. The analytical error performance of the receiver assuming zero inter-symbol interference (ISI) and inter-path interference (IPI) is analyzed in Section III. In Section IV we provide numerical examples including assessments of the impacts of ISI and IPI caused by frequency-selective fading, followed by concluding remarks in Section V.

II. SYSTEM MODEL

Notation: Boldface upper-case and lower-case letters represent, respectively, matrices and column vectors. Temporal indexes such as l (resolvable path) are put in parentheses next to a variable. Spatial indexes such as n (transmit antenna) and m (receive antenna) are indicated by subscripts. Operations to a vector, a matrix, or a scalar are represented by superscripts. These superscripts include $(\cdot)^\dagger$ representing conjugate transpose, $(\cdot)^*$ representing complex conjugate, $(\cdot)'$ representing transpose, and $(\cdot)^+$ representing pseudoinverse.

A. Transmitter model

We consider a single-user system with N transmit and M receive antennas in a frequency-selective Rayleigh fading channel with additive white Gaussian noise (AWGN). In the transmitter, input data are first serial-to-parallel converted into N streams without space-time encoding. Each of the N streams of symbols is then baseband modulated. Finally the N streams of waveforms are sent to N transmit antennas for simultaneous transmission.

We focus on the baseband model of a system employing pulse amplitude modulation (PAM) with zero inter-symbol interference design¹. The n^{th} transmitted data stream (the signal from the n^{th} transmit antenna) is expressed as

$$x_n(t) = \sqrt{E_s} \sum_{k=-\infty}^{\infty} s_n(k)g(t - kT), \quad n = 1, \dots, N \quad (1)$$

where $s_n(k)$ is the k^{th} symbol of the n^{th} data stream, E_s is the energy per symbol, T is the symbol interval, and $g(t)$ is the transmitted Nyquist pulse shape (same for all transmitted symbols) whose energy is normalized so that $\int_{-\infty}^{\infty} g^2(t)dt = 1$. In practical systems, frequency-selective fading occurs when

¹Although the pulse shape is designed to have zero ISI at sampling instants, multipath delay may cause ISI.

the transmitted signals are of wide bandwidth. A widely used method to generate a wide-bandwidth signal is by applying direct-sequence spreading to the transmitted symbols. In this case, $g(t)$ is the spread waveform and each chip is shaped by a Nyquist pulse shaping filter.

B. Receiver model

1) *Received signal*: Each of the N transmitted signals is propagated independently through a frequency-selective Rayleigh fading channel and received also independently by all M receive antennas. Fading is assumed to be quasistatic [9] allowing the channel fading process to be constant over a block of data and change independently to a new realization. With this assumption, the widely used model for the impulse response of a frequency-selective Rayleigh fading channel can be expressed as [10]

$$c(t) = \sum_{l=0}^{L-1} h(l)\delta(t - lT_p) \quad (2)$$

where $h(l)$ (zero-mean complex Gaussian) represents the Rayleigh fading coefficient for the l^{th} path, T_p is the minimum multipath resolution, L is the number of resolvable multipath components, and $\delta(t)$ is the Dirac delta function. The channel is also modeled as having an exponentially decaying power delay profile. Thus, the average power of the path with index l is related to that of the first path as $E\{|h(l)|^2\} = E\{|h(0)|^2\}e^{-\sigma l}$, where σ is the power decay factor.

The signal from each antenna goes through the frequency-selective channel modeled by Eq. (2), resulting in multiple delayed and independently faded copies of the same signal at the receiver. The received signal of the m^{th} antenna $r_m(t)$, $m = 1, \dots, M$, is a sum of signals from N transmit antennas and is expressed as

$$r_m(t) = \sum_{n=1}^N \sum_{l=0}^{L-1} h(l)_{mn} x_n(t - lT_p) + \nu_m(t) \quad (3)$$

where $h(l)_{mn}$ represents the channel fading coefficient of the l^{th} path for the signal from the n^{th} transmit antenna to the m^{th} receive antenna, $\nu_m(t)$ is the white Gaussian noise process (complex with a zero mean) of power spectral density N_0 , and $x_n(t)$ was given in (1).

The received signal $r_m(t)$ is filtered by a matched filter matched to $g(t)$ and then sampled at the symbol rate of each data stream. In the case when $g(t)$ is a direct sequence spread waveform, $r_m(t)$ should be filtered by a chip matched filter and sampled at the chip rate and then despread. The output of the matched filter is processed by an array processing unit to separate signals from the N transmit antennas on a path-by-path basis. A RAKE receiver then captures the energy contained in the resolvable multipath components and forms the decision statistics for symbol-by-symbol detection of each of the N parallel streams of data.

In deriving the following discrete model of the system, symbol index k will be omitted for simplicity of notation. In the absence of inter-symbol and inter-path interference, the received spatial signal vector at the matched filter output for

the l^{th} path of a symbol, $\mathbf{r}(l)$ ($M \times 1$), is expressed as

$$\mathbf{r}(l) = [r_1, r_2, \dots, r_M]^T \sqrt{E_s} \mathbf{H}(l) \mathbf{s} + \boldsymbol{\nu}(l), \quad l = 0, \dots, L-1 \quad (4)$$

where r_m is the received signal from the m^{th} receive antenna, $\mathbf{s} = [s_1, s_2, \dots, s_N]^T$ is the transmitted symbol vector over one symbol interval across N transmit antennas, and $\boldsymbol{\nu}(l) = [\nu_1(l), \nu_2(l), \dots, \nu_M(l)]^T$ is the received wide-sense stationary noise vector with independent and identically distributed components on the l^{th} path. The channel matrix for the l^{th} path of a particular symbol, $\mathbf{H}(l)$ ($M \times N$), can be expressed as

$$\mathbf{H}(l) = [\mathbf{h}(l)_1 \ \mathbf{h}(l)_2 \ \dots \ \mathbf{h}(l)_N] \\ = \begin{bmatrix} h(l)_{11} & h(l)_{12} & \dots & h(l)_{1N} \\ h(l)_{21} & h(l)_{22} & \dots & h(l)_{2N} \\ \vdots & \vdots & \ddots & \vdots \\ h(l)_{M1} & h(l)_{M2} & \dots & h(l)_{MN} \end{bmatrix} \quad (5)$$

where the zero-mean, Gaussian column vector $\mathbf{h}(l)_n$ ($M \times 1$) is given as $\mathbf{h}(l)_n = [h(l)_{1n}, h(l)_{2n}, \dots, h(l)_{Mn}]^T$.

Symbol vector \mathbf{s} is detected using the received spatial vectors on L resolvable paths $\mathbf{r}(l)$, $l = 0, \dots, L-1$, given in (4). Because of the inter-antenna interference, $\mathbf{r}(l)$ needs to be processed before multipath combining.

2) *Zero-forcing processing*: A ZF scheme is applied to separate the transmitted symbols from all transmit antennas on a path-by-path basis. The reason that the ZF scheme is chosen is because the performance of the ZF receiver approaches that of the MMSE scheme at high signal-to-noise ratios (SNR) [1] [9] and it is easier to analyze the ZF structure. In the ZF receiver, the received spatial signal vector on the l^{th} path given by Eq. (4) is pre-multiplied by the pseudoinverse of the channel matrix $\mathbf{H}(l)^+$. Thus, the zero-forced signal of the l^{th} path of a symbol, $\mathbf{y}(l)$ ($N \times 1$), is written as

$$\mathbf{y}(l) = [y(l)_1, y(l)_2, \dots, y(l)_N]^T \\ = \mathbf{H}(l)^+ \mathbf{r}(l) = \sqrt{E_s} \mathbf{s} + \boldsymbol{\xi}(l) \quad (6)$$

where $\boldsymbol{\xi}(l) = \mathbf{H}(l)^+ \boldsymbol{\nu}(l)$ is the zero-mean noise vector. Under the assumption of the quasistatic fading made earlier, the instantaneous noise power on the l^{th} path of a symbol of the n^{th} data stream is $[E\{\boldsymbol{\xi}(l)\boldsymbol{\xi}(l)^\dagger\}]_{nn} = N_0 [\mathbf{H}(l)^+ (\mathbf{H}(l)^+)^{\dagger}]_{nn}$, where $[\cdot]_{nn}$ denotes the $(nn)^{\text{th}}$ component of a matrix and $E\{\cdot\}$ denotes statistical expectation. In the case when $\mathbf{H}(l)^\dagger \mathbf{H}(l)$ is a full rank matrix², it can be easily obtained that $[E\{\boldsymbol{\xi}(l)\boldsymbol{\xi}(l)^\dagger\}]_{nn} = N_0 [(\mathbf{H}(l)^\dagger \mathbf{H}(l))^{-1}]_{nn}$. To simplify notations, let us introduce the following variable (a positive real scalar)

$$\beta(l)_n = \frac{1}{\sqrt{[(\mathbf{H}(l)^\dagger \mathbf{H}(l))^{-1}]_{nn}}} \quad (7)$$

It was shown in [1] that $\beta(l)_n^2 = 1/[(\mathbf{H}(l)^\dagger \mathbf{H}(l))^{-1}]_{nn}$ can be written in a quadratic form as

$$\beta(l)_n^2 = \mathbf{h}(l)_n^\dagger \mathbf{G}(l) \mathbf{h}(l)_n$$

²Such a condition is satisfied when signals from receive antennas are independent or have low correlations, and is assumed true in this paper.

where $\mathbf{G}(l)$, whose eigenvalues are denoted as $\lambda_1 \geq \lambda_2 \geq \dots \geq \lambda_M$, is a Hermitian and non-negative $M \times M$ matrix independent of $\mathbf{h}(l)_n$.

There exists a unitary transformation $\Phi = [\phi_1 \ \phi_2 \ \dots \ \phi_M]$ that can diagonalize $\mathbf{G}(l)$ as $\mathbf{G}(l) = \Phi^\dagger \Lambda \Phi$, where $\Lambda = \text{diag}[\lambda_1, \lambda_2, \dots, \lambda_M]$. Hence $\beta(l)_n^2$ can be expressed as

$$\beta(l)_n^2 = \mathbf{h}(l)_n^\dagger \Phi^\dagger \Lambda \Phi \mathbf{h}(l)_n = \mathbf{f}(l)^\dagger \Lambda \mathbf{f}(l) \quad (8)$$

where $\mathbf{f}(l) = \Phi \mathbf{h}(l)_n$. Because $h(l)_{mn}$ with different indexes (m , n , and l) are independent, zero-mean, complex Gaussian random variables, $f(l)_i$ (the i^{th} element of $\mathbf{f}(l)$), being a linear combination of $h(l)_{1n}, \dots, h(l)_{Mn}$, is a complex Gaussian random variable with $E\{f(l)_i\} = 0$. Because Φ is unitary, it is normal, i.e., $\Phi^\dagger \Phi = \Phi \Phi^\dagger = \mathbf{I}_M$ where \mathbf{I}_M is the $M \times M$ identity matrix. Hence

$$\begin{aligned} E\{\mathbf{f}(l)\mathbf{f}(l)^\dagger\} &= E\{\Phi \mathbf{h}(l)_n \mathbf{h}(l)_n^\dagger \Phi^\dagger\} \\ &= \Phi e^{-\sigma l} \mathbf{I}_M \Phi^\dagger = e^{-\sigma l} \mathbf{I}_M. \end{aligned}$$

Examining only the i^{th} and j^{th} elements of $\mathbf{f}(l)$, it is found

$$E\{f(l)_i f(l)_j^*\} = e^{-\sigma l} \delta(i-j) \quad (9)$$

where $\delta(i-j)$ is defined as

$$\delta(i-j) = \begin{cases} 1, & \text{for } i=j \\ 0, & \text{otherwise.} \end{cases}$$

Thus, $f(l)_i$, $l = 1, \dots, L-1$, $i = 1, \dots, M$, are uncorrelated, and therefore statistically independent random variables because they are Gaussian. Applying $i=j$ to (9), we obtain

$$E\{f(l)_i f(l)_i^*\} = E\{|f(l)_i|^2\} = e^{-\sigma l}. \quad (10)$$

From Eqs. (8) and (9) it can be easily seen that $\beta(l)_n$, $l = 0, 1, \dots, L-1$, are nonnegative real and independent from one another because fading processes are independent for different resolvable multipath components. It was shown in [1] that the eigenvalues of $\mathbf{G}(l)$ are either 1 or 0, with exactly $D = M - N + 1$ eigenvalues equal to 1. Thus, $\lambda_1 = \dots = \lambda_D = 1$ and $\lambda_{D+1} = \dots = \lambda_M = 0$. Because $|f(l)_i|$ is Rayleigh and $|f(l)_i|^2$ is chi-square distributed with two degrees of freedom, it is easy to determine that $\beta(l)_n^2$ is chi-square distributed with $2D = 2(M - N + 1)$ degrees of freedom and can be rewritten as

$$\beta(l)_n^2 = \sum_{i=1}^M \lambda_i f(l)_i f(l)_i^* = \sum_{d=1}^D f(l)_d f(l)_d^*. \quad (11)$$

The noise components of the L zero-forced signals carrying the same symbol as given in Eq. (6) have different power for different path index l . In order to derive the coefficients for maximal ratio combining, we further process the zero-forced signals as follows. Let us define an $N \times N$ diagonal matrix

$$\mathbf{K}(l) = \text{diag}[\beta(l)_1, \beta(l)_2, \dots, \beta(l)_N]. \quad (12)$$

The processed spatial signal vector for the l^{th} path over a symbol interval, $\mathbf{z}(l)$ ($N \times 1$), is written as

$$\begin{aligned} \mathbf{z}(l) &= [z(l)_1, z(l)_2, \dots, z(l)_N]' \\ &= \mathbf{K}(l) \mathbf{y}(l) = \sqrt{E_s} \mathbf{K}(l) \mathbf{s} + \boldsymbol{\varepsilon}(l) \end{aligned} \quad (13)$$

where

$$\boldsymbol{\varepsilon}(l) = [\varepsilon(l)_1, \varepsilon(l)_2, \dots, \varepsilon(l)_N]' = \mathbf{K}(l) \boldsymbol{\xi}(l) \quad (14)$$

with $[E\{\boldsymbol{\varepsilon}(l)\boldsymbol{\varepsilon}(l)^\dagger\}]_{nn} = N_0$, independent of path index l . Notice that although matrix $\mathbf{K}(l)$ is positive and real, the noise vector $\boldsymbol{\varepsilon}(l)$ is complex.

3) *Multipath combining*: We focus on detecting a particular symbol of the n^{th} data stream. We extract the MIMO processed signals (from Eq. (13)) on all L paths, which carry the same symbol of the n^{th} data stream, and write them in an $L \times 1$ temporal vector as

$$\begin{aligned} \mathbf{z} &= [z(0)_n, z(1)_n, \dots, z(L-1)_n]' \\ &= \left[\sqrt{E_s} \beta(0)_n s_n + \varepsilon(0)_n, \dots, \right. \\ &\quad \left. \sqrt{E_s} \beta(L-1)_n s_n + \varepsilon(L-1)_n \right]'. \end{aligned} \quad (15)$$

The decision variable for the symbol can be obtained by combining all L elements of \mathbf{z} . The MRC weight vector $\boldsymbol{\beta}$ is chosen according to the SNR on each path. From (13), such a weight is determined to be

$$\boldsymbol{\beta} = [\beta(0)_n, \beta(1)_n, \dots, \beta(L-1)_n]'. \quad (16)$$

Therefore, the decision variable for any symbol of the n^{th} data stream is expressed as³

$$\lambda_n = \Re\{\boldsymbol{\beta}^\dagger \mathbf{z}\} \quad (17)$$

where $\Re\{\cdot\}$ denotes the real part.

III. ERROR PERFORMANCE

We will focus on binary phase-shift keying (BPSK) for which $s_n \in (-1, 1)$ with equal probability to take on the values of 1 and -1. The analysis for quadriphase-shift keying (QPSK) is essentially the same and the results can be extended to other PAM schemes. We assume that the transmitted bit is a 1 ($s_n = 1$) and determine the conditional probability of error. With $P(-1) = P(1)$, the average BER is the same as the BER conditioned on $s_n = 1$.

By applying \mathbf{z} given in (15) and $\boldsymbol{\beta}$ in (16), and replacing symbol energy E_s with bit energy E_b , we write $\boldsymbol{\beta}^\dagger \mathbf{z}$ conditioned on $s_n = 1$ as

$$\begin{aligned} \boldsymbol{\beta}^\dagger \mathbf{z} &= \left(\sqrt{E_b} \beta(0)_n^2 + \beta(0)_n \varepsilon(0)_n \right) + \dots + \\ &\quad \left(\sqrt{E_b} \beta(L-1)_n^2 + \beta(L-1)_n \varepsilon(L-1)_n \right). \end{aligned} \quad (18)$$

The instantaneous SNR on the l^{th} path (the l^{th} term on the right-hand side of (18)) is obtained as $\gamma(l) = \frac{E_b}{N_0} \beta(l)_n^2$. Substituting $\beta(l)_n^2$ given in (11) into the above expression yields another form of $\gamma(l)$ as

$$\gamma(l) = \frac{E_b}{N_0} \sum_{d=1}^D |f(l)_d|^2 \quad (19)$$

where $f(l)_d$, $l = 0, \dots, L-1$, $d = 1, \dots, D$, as analyzed and concluded earlier, are zero-mean and independent Gaussian random variables. More analysis on the noise component contained in the l^{th} term on the right-hand side of (18) reveals

³Notice that $\boldsymbol{\beta}$ is a real vector because $\beta(l)$, $l = 0, \dots, L-1$, are all real.

that it has a zero mean with an instantaneous variance also equal to a sum of D independent variables. Thus, the l^{th} term on the right-hand side of (18) is equivalent to a D -branch spatial diversity system employing MRC in a frequency-nonselctive Rayleigh fading channel [10]. The ZF receiver for a MIMO system with N transmit antennas and M receive antennas over a frequency-selective Rayleigh fading channel with L resolvable multipath components is transformed into a 2-dimensional RAKE with a diversity order of DL (D times L). Every element of the D -branch group has the same average SNR but the average SNRs for the L groups are different except when the channel power decay factor σ given in (10) is equal to zero.

The combined instantaneous SNR per bit is given by

$$\gamma_b = \frac{E_b}{N_0} \sum_{l=0}^{L-1} \sum_{d=1}^D |f(l)_d|^2. \quad (20)$$

The probability of error conditioned on a fixed set of $\{f(l)_d\}$ is a Q -function and is given as $P_b(\gamma_b) = Q(\gamma_b)$. If $p(\gamma_b)$, the probability density function (PDF) of γ_b , is obtained, the average BER can be calculated as $P_b = \int_0^\infty p(\gamma_b) P_b(\gamma_b) d\gamma_b$.

When $f(l)_d$, $l = 0, \dots, L-1$, $d = 1, \dots, D$ are independent and identically distributed or when they are independently distributed but with distinct mean-square values, a closed-form expression for the PDF of γ_b is feasible [10]. For the problem being addressed in this paper, however, the mean-square values of $f(l)_d$ are neither all identical nor completely unique. Finding the PDF of γ_b using the PDF-based approach for this case becomes intractable. An easier approach to obtain the average bit error rate is to use the moment-generating function (MGF) based approach [11]. In this approach, the Gaussian Q -function is first expressed in the form as $Q(x) = \frac{1}{\pi} \int_0^{\pi/2} \exp\left(-\frac{x^2}{2 \sin^2 \phi}\right) d\phi$, $x \geq 0$. Based on (20), the average BER for Rayleigh fading channels derived using the MGF-based approach is given as [11]

$$P_b = \frac{1}{\pi} \int_0^{\pi/2} \prod_{l=0}^{L-1} \left(1 + \frac{\bar{\gamma}(l)_d}{\sin^2 \phi}\right)^{-D} d\phi \quad (21)$$

where $\bar{\gamma}(l)_d = \frac{E_b}{N_0} E\{|f(l)_d|^2\}$.

IV. NUMERICAL EXAMPLES AND DISCUSSION

In all simulations, the MIMO processing and maximal ratio combining follow exactly the procedures presented in Section II. The matrix channel coefficients are generated according to the quasistatic model. Elements of the channel matrix (5) are independent, complex, Gaussian random variables. This corresponds to practical situations where all transmit and receive antennas are sufficiently separated. In order to approximate the Rayleigh statistics well, the number of blocks (not the total number of bits) for the quasistatic fading to be simulated must be sufficiently large.

Normalization for all numerical examples is done as follows. When there are L resolvable multipath components, average power of the first path ($l = 0$) is normalized to 1 and the relative average power of the path with index l to the first path is $e^{-\sigma l}$. Error performance is evaluated for the transmitted data stream with index $n = 1$. For the system with

N transmit antennas, M receive antennas, and L resolvable paths, SNR per bit in dB is defined as

$$\theta_b = \frac{E_b}{N_0} (\text{dB}) + 10 \log_{10}(D) + 10 \log_{10} \left(\sum_{l=0}^{L-1} e^{-\sigma l} \right).$$

The term $10 \log_{10}(D)$ above is added to account for difference between the number of receive and transmit antenna elements. The term $10 \log_{10} \left(\sum_{l=0}^{L-1} e^{-\sigma l} \right)$ is used to compensate for the extra power contained in multiple resolvable paths.

Analytical and simulated (with marks) error performance curves of the system with different combinations of M , N , and L in the absence of ISI and IPI are shown in Fig. 1. For all cases evaluated, the analytical and simulated error rate

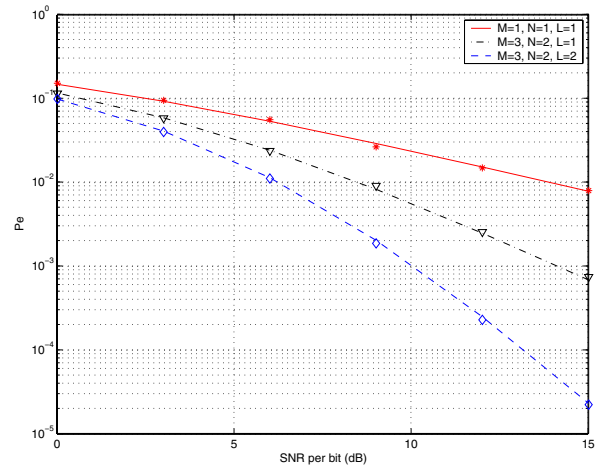


Fig. 1. Analytical and simulated (with marks) error performance curves with different system parameters.

curves match very well. The diversity order of 1, 2, and 4 for, respectively, $(M, N, L) = (1, 1, 1)$, $(3, 2, 1)$, and $(3, 2, 2)$ can be clearly seen from Fig. 1.

The analytical probability of error given in (21) is based on the assumption that there is no inter-symbol interference or inter-path interference. Therefore, results based on the analytical expression given in (21) can be considered as the performance lower bound for a MIMO system with a ZF receiver combined with an MRC in a frequency-selective Rayleigh fading channel. When ISI and IPI caused by multipath are considered, an analytical expression for the average BER is difficult to obtain because it depends on the waveform $g(t)$ applied. We provide simulation results to assess the effects of ISI and IPI caused by multipath for a MIMO system with direct-sequence spreading. One direct-sequence spreading code is applied to spread symbols from all transmit antennas⁴. In this case, $g(t)$ given in (1) is a spread waveform and the multipath resolution T_p given in (2) is equal to one chip interval. For the numerical examples provided, the 32nd Walsh code of length 64 (spreading factor SF=64) is applied to spread

⁴If multiple spreading codes are used, signals transmitted simultaneously from multiple antennas could have been separated by exploiting the different codes as in a code-division multiple-access system. This is not the general purpose of MIMO systems and is not pursued in this paper.

transmitted symbols. Each chip is pulse shaped by a square-root raised cosine (RRC) filter with a roll-off factor of 0.3. The received signal is filtered by a chip matched filter (also an RRC filter with a roll-off factor of 0.3), sampled at the chip rate and despread. Because the relative delay between two resolvable multipath components is an integer multiple of one chip duration, frequency-selective fading does not cause inter-chip interference in this design. The nonorthogonality between a code and its shifted version, however, does cause IPI. Simulated error performance curves with $M = 3$, $N = 2$, $L = 2$ are shown in Fig. 2. For comparison purposes, the

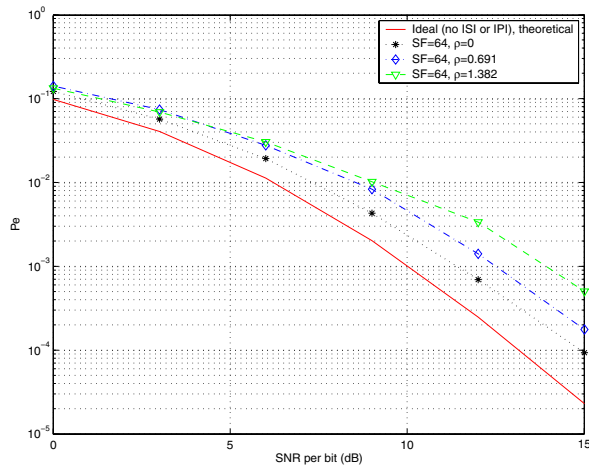


Fig. 2. Simulated error performance curves in the presence of ISI and IPI ($M = 3$, $N = 2$, $L = 2$).

curve with the same set of parameters under the assumption of zero ISI and IPI is also plotted in the same figure. For an uncoded system with $M = 3$, $N = 2$, $L = 2$, $\sigma = 0$ and other system parameters chosen, the performance degradation caused by ISI and IPI is about 1.4dB at $P_b = 10^{-3}$.

To assess the impacts of the number of resolvable paths L , we simulated BER curves for a system with $M = 3$, $N = 2$, $\sigma = 0$, and $L = 2, 3$, and 4. These curves are plotted in Fig. 3 together with the theoretical BER lower bound. Contrary to what we might have normally anticipated, performance gets worse when L increases. This is because that the gain in energy from more multipath components for a larger L are compensated in the expression of SNR per bit adopted and the diversity gain from $L = 2$ (4^{th} -order effective path diversity) to $L = 4$ diminishes. However, increasing L may significantly increase⁵ the level of ISI and IPI.

V. CONCLUSION

We have provided details of the signal processing procedures for a MIMO system with a ZF receiver combined with an MRC in frequency-selective Rayleigh fading channels. We have also derived the analytical error rate expression as a function of E_b/N_0 , number of resolvable paths L , number of transmit and receive antenna elements (N, M), and channel power decay factor σ under the assumption of zero ISI

⁵This depends on the spreading code applied, especially the autocorrelation property of the code.

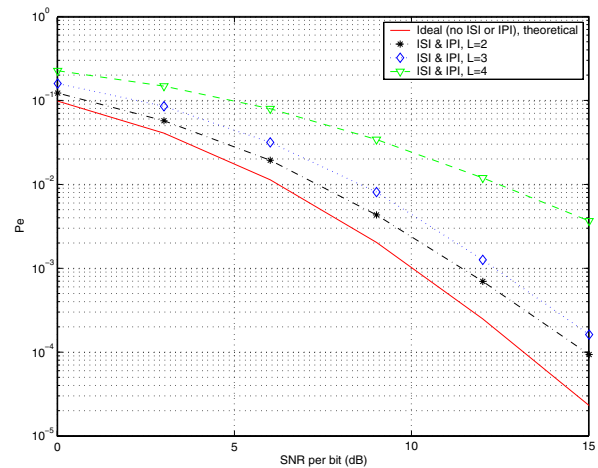


Fig. 3. Effects of number of resolvable paths ($M = 3$, $N = 2$, $\sigma = 0$).

and IPI. The ZF receiver with maximal ratio combining for an (N, M) MIMO system in a frequency-selective Rayleigh fading channel with L resolvable multipath components is equivalent to a 2-dimensional RAKE with a diversity order of $(M - N + 1)L$. The effects of ISI and IPI caused by frequency-selective fading have been studied by simulations for a system with direct-sequence spreading applied to all transmitted symbols. When the transmitted wideband signals are generated by direct-sequence spreading with a spreading factor of 64, numerical results suggest that ISI and IPI may cause significant performance degradation.

REFERENCES

- [1] J. H. Winters, J. Salz, and R. D. Gitlin, "The impact of antenna diversity on the capacity of wireless communications systems," *IEEE Trans. on Communications*, vol. 42, pp. 1740–1751, Feb./Mar./Apr. 1994.
- [2] J. H. Winters, "On the capacity of radio communication systems with diversity in a Rayleigh fading environment," *IEEE Journal on Selected Areas in Communications*, vol. SAC-5, pp. 871–878, June 1987.
- [3] G. J. Foschini and M. J. Gans, "On limits of wireless communications in a fading environment when using multiple antennas," *Wireless Personal Communications*, pp. 311–335, 1998.
- [4] P. F. Driessen, "On the capacity formula for multiple input-multiple output wireless channels: A geometric interpretation," *IEEE Trans. on Communications*, vol. 47, pp. 173–176, Feb. 1999.
- [5] R. S. Blum, J. H. Winters, and N. R. Sollenberger, "On the capacity of cellular systems with MIMO," *IEEE Communications Letters*, vol. 6, pp. 242–244, June 2002.
- [6] R. S. Blum and J. H. Winters, "On the optimum MIMO with antenna selection," *IEEE Communications Letters*, vol. 6, pp. 322–324, Aug. 2002.
- [7] G. D. Golden, C. J. Foschini, R. A. Valenzuela, and P. W. Wolniansky, "Detection algorithm and initial laboratory results using V-blast space-time communication architecture," *Electronics Letters*, vol. 35, pp. 14–16, Jan. 1999.
- [8] G. Bauch and J. Hagenauer, "Smart versus dumb antennas-capacities and FEC performance," *IEEE Communications Letters*, vol. 6, pp. 55–57, Feb. 2002.
- [9] D. A. Gore, R. W. Heath, Jr., and A. J. Paulraj, "Transmit selection in Spatial multiplexing systems," *IEEE Communications Letters*, vol. 6, pp. 491–493, Nov. 2002.
- [10] J. G. Proakis, *Digital Communications (ch. 14)*. New York, NY: McGraw-Hill, 3rd ed., 1995.
- [11] M. K. Simon and M.-S. Alouini, "A unified approach to the performance analysis of digital communication over generalized fading channels," *Proceedings of the IEEE*, vol. 86, pp. 1860–1877, Sep. 1998.
- [12] M. Schwartz, W. R. Bennett, and S. Stein, *Communication systems and techniques*. Piscataway, NJ: IEEE Press, 1995.